Journal of Magnetism and Magnetic Materials 410 (2016) 41–46

Contents lists available at ScienceDirect

Journal of Magnetism and Magnetic Materials

journal homepage: www.elsevier.com/locate/jmmm

Buckminsterfullerene's movability on the Fe(001) surface

Alexander A. Kuzubov [a,b], Evgenia A. Kovaleva [a,*], Pavel V. Avramov [c], Anastasia S. Kholtobina [a], Natalya S. Mikhaleva [a], Artem V. Kuklin [a,c]

[a] Siberian Federal University, 79 Svobodny pr., Krasnoyarsk 660041, Russia
[b] L.V. Kirensky Institute of Physics, 50 Akademgorodok, Krasnoyarsk 660036, Russia
[c] Kyungpook National University, 80 Daehakro, Bukgu, Daegu 41566, South Korea

ARTICLE INFO

Article history:
Received 23 October 2015
Received in revised form
24 February 2016
Accepted 4 March 2016
Available online 5 March 2016

Keywords:
Buckminsterfullerene
C_{60}
Fe(001)
Spintronics
Adsorption
Relocation
DFT

ABSTRACT

Organic-based spintronics is one of the most fast-developing fields in nanoelectronics. Buckminsterfullerene-based composites are widely investigated due to its unique properties and there is a number of studies concerned with its interfaces with various types of substrates. Ferromagnetic surfaces are of a particular interest for potential spintronics applications. Based on the data reported in literature, we suppose that there are more than one stable structure in C_{60}/Fe(001) composite system. Here we investigate different possible adsorption sites of C_{60} molecule and reveal the possibility of their coexistence and its influence on the composite properties.

1. Introduction

Interfaces of ferromagnetic materials with organic molecules are of great interest due to the promising contact-induced changes in their electronic and magnetic properties which enable using them in various type of spintronic devices [1–3]. C_{60} is considered as a promising material for organic electronics devices such as spin valves etc [4–8]. Films of C_{60} deposited on various noble and other closed-pack metal surfaces have been thoroughly studied both theoretically and experimentally [9–14]. Low-energy electron diffraction (LEED) analysis was found to be an efficient tool for defining structural parameters of interfaces [9,10,12]. These results are also supported by the density functional calculations. Formation of one or even several-atom vacancies due to the fullerene adsorption was reported in some cases [9,12,14,15] allowing tuning the interface properties by altering synthesis conditions. Recent studies of C_{60} films on Fe(001) surface reveal significant hybridization between fullerene π-states and iron 3d orbitals [16,17] leading to the change in charge and spin distribution in the contact area. Fullerene gets some degree of spin polarization opposite to that of the substrate. There are two different structures defined to be the most stable in this system being quite close to each other both in geometry of C_{60}/Fe(001) mutual arrangement and adsorption energy [15,17]. We then suppose the coexistence of these two and, probably, some more structures. This study is to shed the light on the possibility of such multiple deposition of C_{60} on iron surface.

2. Computational method

The first-principles density functional theory calculations of C60/Fe(100) composites were performed using VASP code [18–21]. GGA PBE potential [22,23] and projector augmented wave [24,25] method (PAW) were implemented. Geometry optimization was performed until the forces acting on atoms were less than 0.01 eV/Å.

First, unit cell of bulk Fe was optimized. Then Fe(100) surface was constructed by cutting it along the corresponding crystallographic plane. In order to simulate C60/Fe(100) composites, we used 4×4 supercell of iron surface. This means that distance between the carbon cages of two neighboring fullerenes ($\sim$4.34 Å) is considerably close to that of the solid fullerene (3.13 Å) [26,27]. Setting the smaller iron substrate is not reasonable since the distance between C60 molecules would be less than that of the solid C60. This, in turn, would lead to the overbinding between neighboring molecules which, in fact, should be bonded via weak van-der-Waals forces. Since the interaction between iron surface and C60 is supposed to involve strong chemical bonding and charge redistribution [15–17], we then consider van-der-Waals supply to be negligible and do not use any correction for it. Artificial

* Corresponding author.
E-mail address: kovaleva.evgeniya1991@mail.ru (E.A. Kovaleva).

http://dx.doi.org/10.1016/j.jmmm.2016.03.023
0304-8853/

interactions in periodic boundary conditions were avoided by setting the vacuum interval of approximately 12 Å in direction normal to the interface. Preliminary tests showed that 8 atomic layers are enough for sufficient representing the features of iron slab.

The Mönkhorst–Pack [28] k-point Brilloin sampling was used. The k-point grid contained $3 \times 3 \times 1$ points along a, b and c directions, respectively. The energy cut-off was specified as 400 eV in all calculations.

Energy of bonding between fullerene and Fe(100) slab was estimated as:

$$E_b = E_c - E_f - E_{Me}, \quad (1)$$

where E_c, E_f and E_{Me} are total energies of composite, fullerene and metal slab, respectively.

Deformation energy of fullerene and iron was found as:

$$E_d = E_{comp} - E_{pristine}, \quad (2)$$

where E_{comp} and $E_{pristine}$ correspond to the energy of iron (fullerene) in the composite and the energy of its pristine optimized structure.

3. Results and discussion

Six different possible high-symmetry configurations of C_{60} deposition on the Fe(100) surface were considered as initial structures (see Fig. 1): four ones with carbon hexagon, pentagon, hexagon-hexagon bond or hexagon-pentagon bond placed upon the iron atom, and two ones with 2 or 4 carbon atoms belonging to one hexagon placed directly or nearly upon corresponding 2 or 4 iron atoms. However, most of them then relaxed to one of the following configurations with much lower symmetry: bridge-1 and bridge-2 have the only difference in the degree of metal slab deformation while the orientation of C_{60} is virtually the same (Figs. 2a and b); initial 2C-atop structure is slightly distorted due to the carbon atoms displacement from top positions resulted in 2 corresponding carbon bonds placed upon Fe atoms (see Fig. 2c), and hereafter denoted as 2C-bond; the most symmetric 4C-atop configuration (Fig. 2d) was however the least favorable among all (see Table 1). 2C-bond and 4C-atop structures have almost the same binding energies which is expectable due to their similarity. Much larger energy difference between bridge-1 and bridge-2 may be explained in terms of the deformation energy of iron slab. Indeed, the slab is substantially more distorted in former case which is also confirmed by the value of deformation energy which is by 0.18 eV higher than that of bridge-2 (0.482 and 0.305 eV for bridge-1 and bridge-2, respectively) while difference in binding energy is equal to 0.19 eV. Values of binding energy themselves are high ($\sim$3 eV) which confirms the presence of chemical bonding in the system, in agreement with previous theoretical and experimental data [15–17]. Both bridge-1 and bridge-2 configurations are somewhat similar to the ones reported in literature [15,17] in terms of fullerene's orientation confirming our suggestions about high movability of C_{60} on iron surface.

For each configuration, charge and spin distribution were estimated using Bader charge analysis [29–31] with high-density FFT

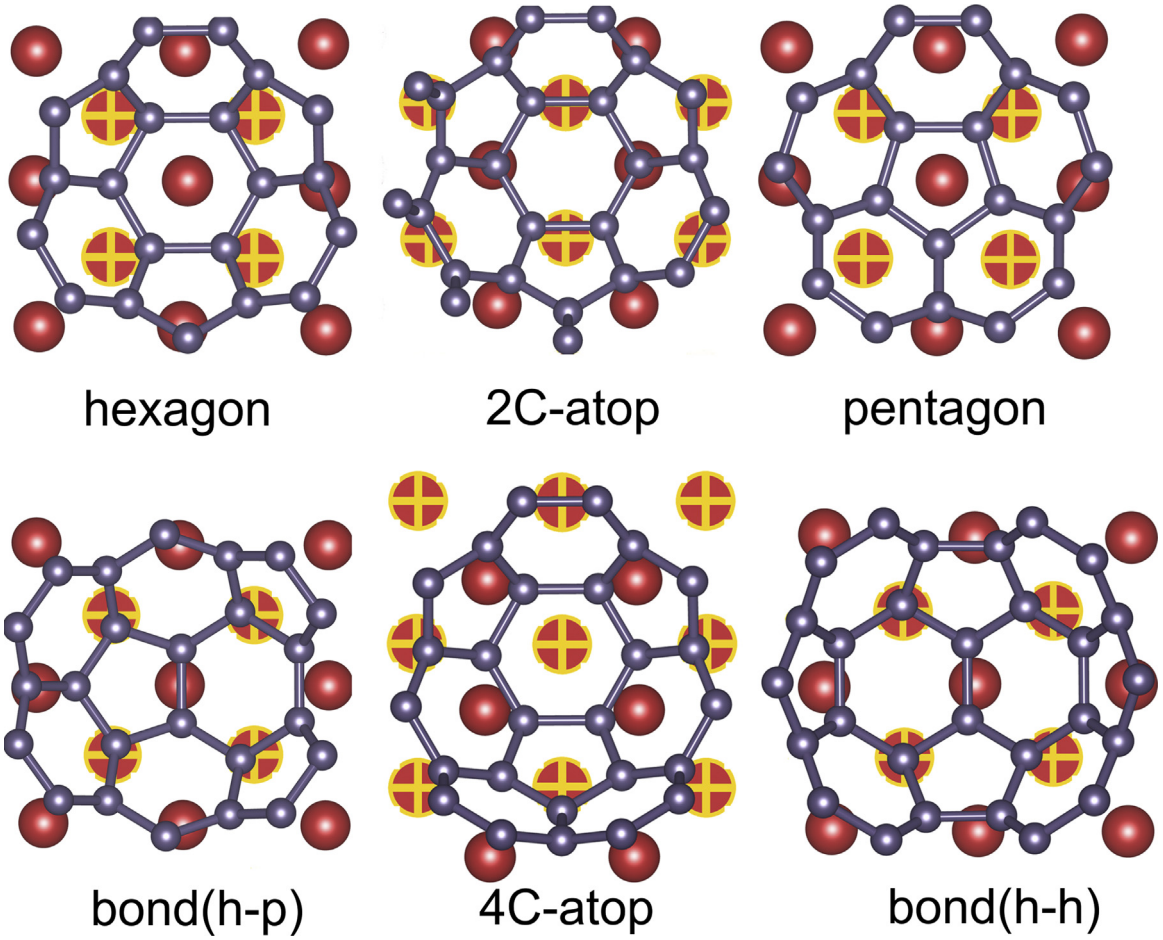

Fig. 1. Initial geometries of C_{60}/Fe(001) interfaces. Carbon atoms are denoted as gray balls, red and yellow–red ones correspond to the first and second layer of iron surface. For the sake of better clarity, only the bottom part of fullerene is presented. (For interpretation of the references to color in this figure legend, the reader is referred to the web version of this article.)

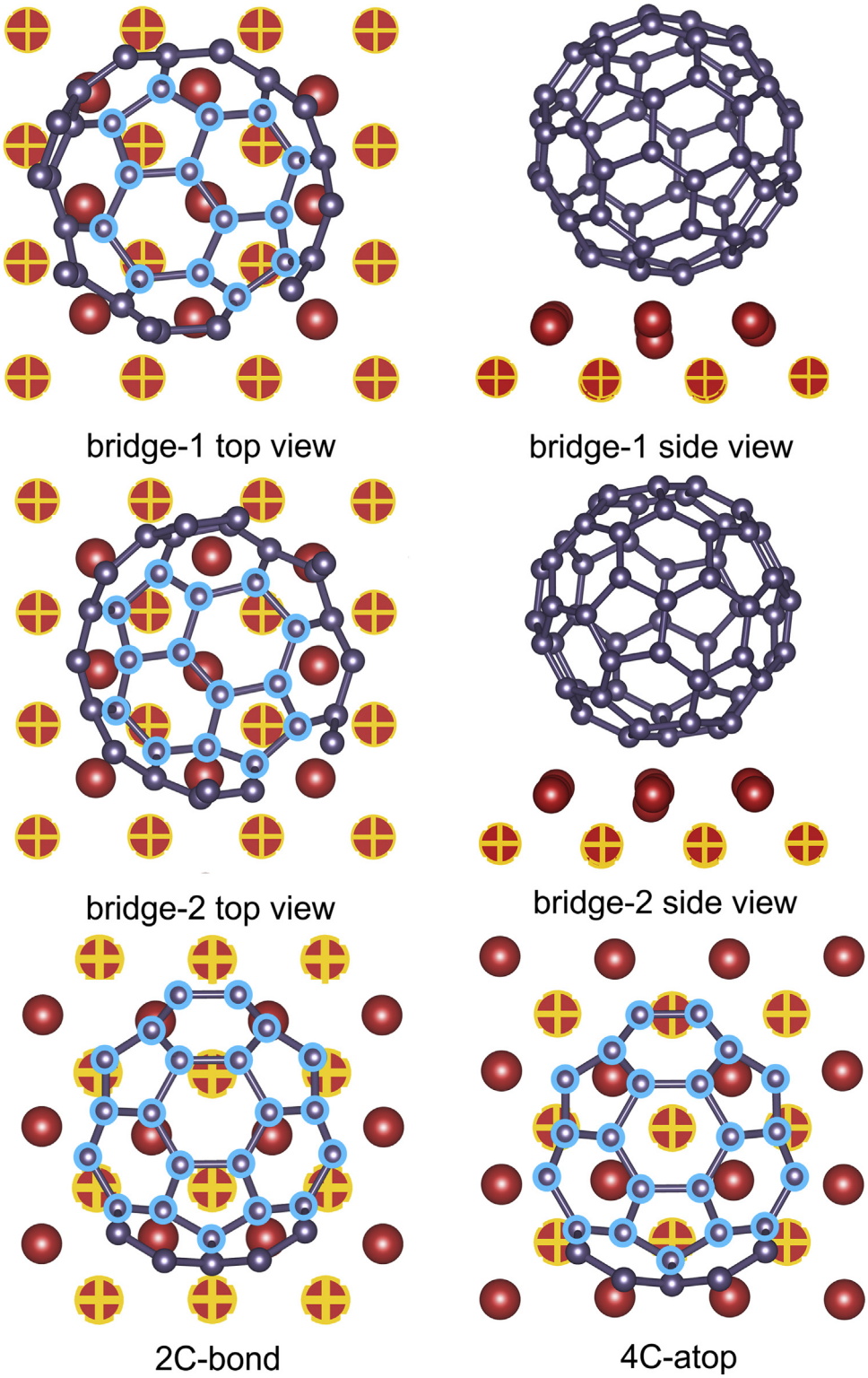

Fig. 2. Geometries of optimized C_{60}/Fe(001) structures. Carbon atoms are denoted as gray balls, red and yellow-red ones correspond to the first and second layer of iron surface. Contacting C_{60} atoms are denoted by blue circles. For the sake of better clarity, only the bottom part of fullerene is presented. (For interpretation of the references to color in this figure legend,the reader is referred to the web version of this article.)

grid (see Table 1). We found magnetic moments to be slightly lower and charge of C_{60} molecule to be slightly higher than that reported in literature [17].This can be attributed to the difference of composite's configurations or to the different density of FFT grid and does not change overall conclusions. Value of spin polarization at Fermi level was calculated as:

$$\xi = \frac{n_{\uparrow} - n_{\downarrow}}{n_{\uparrow} + n_{\downarrow}}, \tag{3}$$

where $n_{\uparrow}$ and $n_{\downarrow}$ are electron densities at Fermi level for spin-up and spin-down states, respectively.

The analysis of partial densities of states (PDOS) shows that electronic structure of C_{60} on the Fe(001) surface is strongly

Table 1
Values of binging energy, charge, magnetic moment and Fermi-level spin polarization in Fe(100)/C_{60} composites.

Configuration	Binding energy (eV)	Total C_{60} charge (e)	Charge on contacting C_{60} atoms (e) (divided by total charge, %)	Magnetic moment of C_{60} molecule (μ_B)	Spin polarization at Fermi level (%)
Bridge-1	−3.082	2.217	2.086 (94.0)	−0.124	−72.6
Bridge-2	−3.274	2.112	2.017 (95.5)	−0.153	38.3
2C-bond	−2.945	1.904	1.554 (86.7)	−0.040	−28.2
4C-atop	−2.921	1.667	1.445 (81.6)	−0.153	51.7

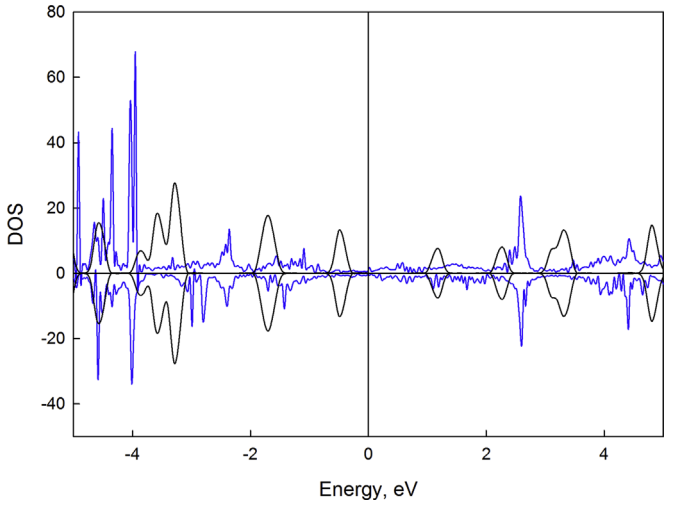

Fig. 3. PDOS of C_{60} molecule for bridge-2 configuration of C_{60}/Fe(001) composite (blue line) in comparison with DOS for pristine fullerene (black line). (For interpretation of the references to color in this figure legend, the reader is referred to the web version of this article.)

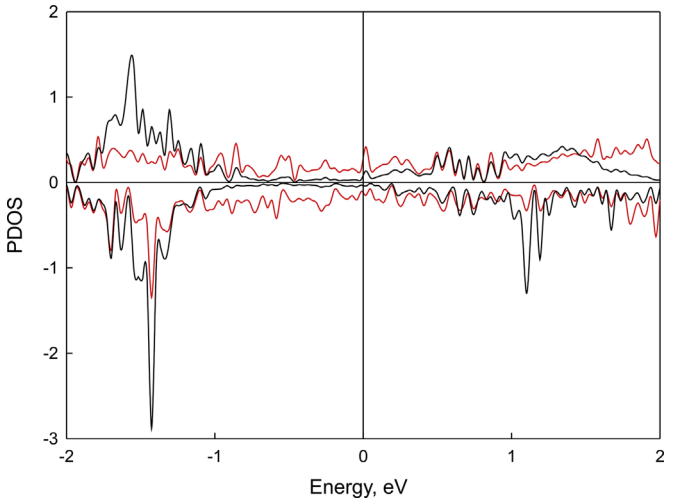

Fig. 4. PDOS of fullerene atoms being in direct contact with iron slab (red line) and atoms from the top part of the fullerene (black line). (For interpretation of the references to color in this figure legend,the reader is referred to the web version of this article.)

distorted comparing with that of the bare fullerene (see Fig. 3). Band gap is vanishing, and peaks are shifted to the lower energies which confirm the major deformation of fullerene playing a key role in composite formation [17]. It should be emphasized that PDOS remains its features both for the atoms being in direct contact with substrate and for the opposite side atoms (Fig. 4). This trend is observed in all four structures we considered. In order to shed the light on the spin density distribution in C_{60}/Fe(100) composites, we present its spatial patterns for each configuration (see Fig. 5). Carbon atoms are negatively spin polarized, and the more is the overlapping between carbon and iron the less is the negative spin density on carbon atom, in perfect agreement with data previously reported [17]. Along with that, total charge on fullerene's molecule is also distributed unequally (see Table 1). We analyzed charges on atoms contacting with iron substrate (14 atoms for bridge-1 and bridge-2 configurations, and 21 atoms for 2C-bond and 4C-atop ones, denoted as blue balls at Fig. 2) and found them to accumulate up to 95.5% of total molecule charge (see Table 1). Bridge configurations are more polarized than more symmetric 2C-bond and 4C-atop, even though the latter ones have more atoms contacting with substrate (contacting atoms were chosen according to the fullerene's curvature in each case).

Since there are several structures being very close to each other, it makes sense to know how easy the fullerene can move from one to another. Potential barriers of fullerene relocation were then calculated using NEB method (see Fig. 6). Even though the lowest barriers correspond to transitions between two familiar configurations, and there is no potential barrier in 2C-bond – bridge-2 transition, other ones are still relatively low (< 0.5 eV) so that fullerene can move freely along the surface.

In order to estimate the movability of C_{60} molecule, rate constant for the transition with the highest potential barrier (bridge-2–4C-atop) was calculated using transition state theory:

$$k = Ae^{-\frac{E_{barrier}}{kT}}, \tag{4}$$

where A was estimated as [32]:

$$A = \frac{kT\prod_{i=1}^{3N-3}\left(1 - e^{-\frac{h\nu_i}{kT}}\right)}{h\prod_{i=1}^{3N-4}\left(1 - e^{-\frac{h\nu_i^{\#}}{kT}}\right)} \tag{5}$$

T is temperature, $E_{barrier}$ is the potential barrier height calculated as the energy difference between transition state and initial composite, nominator product corresponds to the minimum energy points and denominator product corresponds to the transition state, ν_i is the frequency.

Zero-point energy was also taken into account when calculating potential barrier of fullerene's relocation by adding

$$E_i^{\#} = \sum_{i=1}^{3N-4}\frac{h\nu_i^{\#}}{2} \tag{6}$$

to transition state energy and

$$E_0 = \sum_{i=1}^{3N-3}\frac{h\nu_i}{2} \tag{7}$$

to the energy of initial structure. N is the number of atoms in system. Corrected by zero-point energy, potential barrier is equal to 0.468 eV.

According to our calculations, rate constant of C_{60} relocation from bridge-2 to 4C-atop position is equal to 105410 s^{-1} at 300 K and 1521800 s^{-1} at 350 K (A is equal to 7.7×10^{12} s^{-1}). This means that, indeed, even for the highest barrier number of transitions per second is considerably large and should be even larger in other cases so that fullerene can freely move from one structure to another. It should be pointed out that it can adopt not only these four structures but there definitely should be some more configurations, though being very close both in energy and geometry. Indeed, it can be clearly seen from Figs. 1 and 2 that a very small rotation is actually enough to transform, for example, 2C-bond structure to

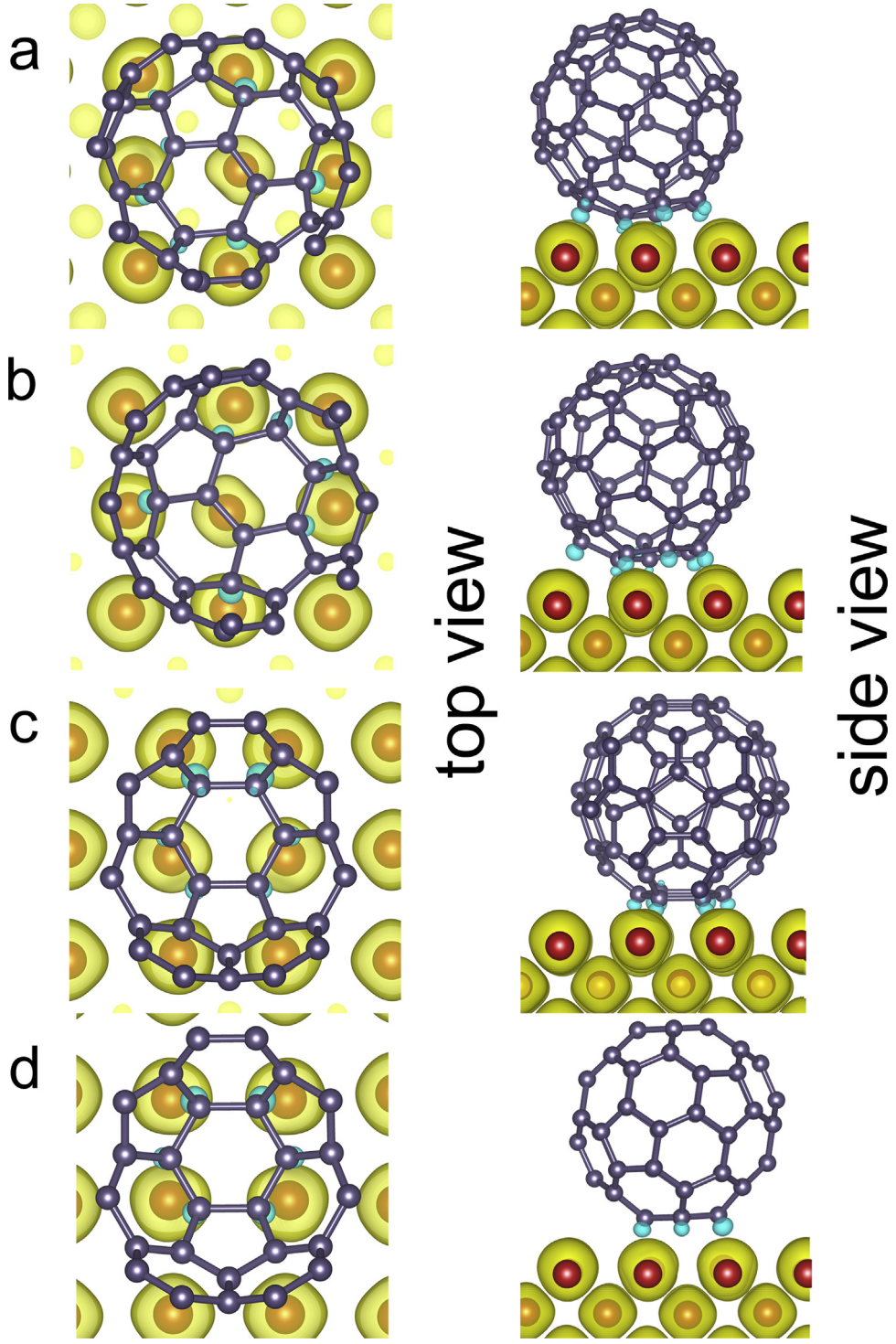

Fig. 5. Spatial distribution of spin density in C_{60}/Fe(001) composites for a) bridge-1; b) bridge-2; c) 2C-bond; d) 4C-atop configurations. Carbon and iron atoms are denoted as gray and red balls, respectively. Yellow (blue) areas correspond to spin-up (spin-down) density. (For interpretation of the references to color in this figure legend, the reader is referred to the web version of this article.)

bridge-2. Another way to go from one configuration to another is to slide along the surface for considerably small distance (e.g. 2C-bond to 4C-atop transition). Thus, the fullerene does not have to move for large distances, which is important since it's not isolated but there are neighboring molecules as well.

Keeping this in mind, we estimated relative probabilities of each state appearance according to the Gibbs distribution at the temperature range of 250–350 K:

$$P_i = \frac{e^{-\frac{E_i}{k_B T}}}{\sum_{i=1}^{4} e^{-\frac{E_i}{k_B T}}}, \tag{8}$$

where E_i is the total energy of configuration i, T is the temperature, and k_B is the Boltzmann constant.

According to the values we obtained (see Table 2), P does not undergo any significant change from 250 to 350 K which is more than enough for nanoelectronic devices working in the narrow

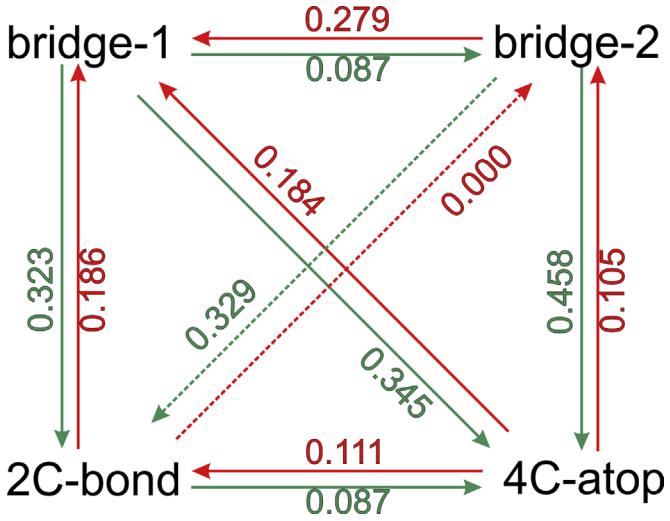

Fig. 6. Potential barriers of C_{60} relocation (eV).

Table 2
Probability (P) of different configurations appearance, charge and magnetic moment versus temperature.

P			
	Temperature (K)		
	250	300	350
Bridge-1	0.252	0.252	0.251
Bridge-2	0.267	0.264	0.262
2C-bond	0.241	0.243	0.244
4C-atop	0.240	0.241	0.243
Averaged properties of C_{60} molecule			
	Temperature (K)		
	250	300	350
Charge (e)	1.982	1.980	1.980
Magnetic moment (μ_B)	−0.119	−0.118	−0.118
Spin polarization at Fermi level (%)	−2.4	−2.5	−2.5

temperature range. It's also worthnoting that all configurations are almost equally probable (~24–27%). This was taken into account when calculating average values of charge transfer, magnetic moment on the C_{60} molecule and its spin polarization at Fermi level:

$$X=P_i \bullet X_i, \quad (9)$$

where X is charge, magnetic moment or spin polarization, i indicates one of the four possible structures, P is the corresponding probability of its appearance. Both charge and magnetic moment were found to remain virtually the same with temperature increase. Stability of these two important characteristics of composite opens perspectives of using C_{60} deposited on Fe(001) as quantum dots, particularly, as possible qubits. Notwithstanding absolute values of spin polarization at Fermi level are relatively large in each case, its average value is only ~2.5% since ξ can be either positive or negative depending on the structure (see Table 1). It does depend on the temperature as well.

4. Conclusion

Density functional study of atomic and electronic structure of C_{60}/Fe(100) composite shows the coexistence of a number of possible structures with strong chemical bonding between composite compartments. Fullerene and slab deformation plays an important role in the formation of composites. Low potential barriers of fullerene's relocation witness the possibility of transitions between stable structures which are almost equally probable according to the Gibbs distribution. Average charge transfer and magnetic moment on C_{60} molecule remain virtually the same within the range of 250–350 K, opening possibility of using such composites for quantum computing or other applications.

Acknowledgment

This work was supported by the Russian Scientific Fund (Project no. 14-13-00139) and the Foundation for Assistance to Small Innovative Enterprises (FASIE) (Project no. 0011742). The authors would like to thank Institute of Computational Modeling of SB RAS, Krasnoyarsk; Joint Supercomputer Center of RAS, Moscow; Center of Equipment for Joint Use of Siberian Federal University, Krasnoyarsk; ICC of Novosibirsk State University and Siberian Supercomputer Center (SSCC) of SB RAS, Novosibirsk for providing the access to their supercomputers.

References

[1] K.V. Raman, Appl. Phys. Rev. 1 (2014) 031101.
[2] S. Sanvito, Nat. Phys. 6 (2010) 562.
[3] N. Atodiresei, et al., Phys. Rev. B 84 (2011) 172402.
[4] D. Çakır, et al., Phys. Rev. B 90 (2014) 245404.
[5] S. Sakai, et al., Appl. Phys. Lett. 91 (2007) 242104.
[6] X. Zhang, et al., Nat. Commun. 4 (2013) 1392.
[7] T.L.A. Tran, et al., Adv. Funct. Mater. 22 (2012) 1180.
[8] M. Gobbi, et al., Org. Electron. 13 (2012) 366.
[9] X.Q. Shi, et al., Phys. Rev. B 84 (2011) 235406.
[10] H.I. Li, et al., Phys. Rev. Lett. 106 (2009) 056101.
[11] L. Tang, et al., Phys. Rev. B 82 (2010) 125414.
[12] G. Xu, et al., Phys. Rev. B 86 (2012) 075419.
[13] X.Q. Shi, et al., J. Mater. Sci. 47 (2012) 7341.
[14] X.Q. Shi, et al., Phys. Rev. B 85 (2012) 075421.
[15] Z.-H. Yang, et al., J. Phys. Chem. C 119 (2015) 10532.
[16] T.L.A. Tran, et al., Appl. Phys. Lett. 98 (2011) 222505.
[17] T.L.A. Tran, et al., ACS Appl. Mater. Interfaces, 5, (2013) 837.
[18] G. Kresse, J. Furthmüller, Comput. Mat. Sci 6 (1996) 15.
[19] G. Kresse, J. Furthmüller, Phys. Rev. B 54 (1996) 11169.
[20] G. Kresse, J. Hafner, Phys. Rev. B 47 (1993) 558.
[21] G. Kresse, J. Hafner, Phys. Rev. B 49 (1994) 14251.
[22] J.P. Perdew, et al., Phys. Rev. B 46 (1992) 6671.
[23] J.P. Perdew, et al., Phys. Rev. B 48 (1993) 4978.
[24] P.E. Blochl, Phys. Rev. B 50 (1994) 17953.
[25] G. Kresse and D. Joubert, Phys. Rev. B 59 (1999) 1758.
[26] Kratschmer, et al., Nature 347 (1990) 354.
[27] H.J. Monkhorst, J.D. Pack, Phys. Rev. B 13 (1976) 5188.
[28] S. Liu, et al., Science 254 (1991) 408.
[29] W. Tang, E. Sanville, G. Henkelman, J. Phys. : Condens. Matter 21 (2009) 084204.
[30] E. Sanville, S.D. Kenny, R. Smith, G. Henkelman, J. Comp. Chem 28 (2007) 899.
[31] G. Henkelman, A. Arnaldsson, H. Jónsson, Comput. Mater. Sci. 36 (2006) 254.
[32] G.H. Vineyard, J. Phys. Chem. Solids 3 (1) (1957) 121.